Available online at www.sciencedirect.com

ScienceDirect

Advances in Space Research xx (2021) xxx-xxx

ADVANCES IN SPACE RESEARCH (a COSPAR publication)

www.elsevier.com/locate/asr

Monitoring River Water Level Using Multiple Bounces of Bridges in SAR images

Xue Chen[a,b], Yueze Zheng[a,c], Junhuan Peng[a,d], Mario Floris[b,*]

[a] *School of Land Science and Technology, China University of Geosciences, Beijing 100083, China*
[b] *Department of Geosciences, University of Padua, Padua 35131, Italy*
[c] *Beijing Institute of Surveying and Mapping, Beijing 100038, China*
[d] *Shanxi Key Laboratory of Resource, Environment and Disaster Monitoring, Jinzhong 245099, China*

Received - March 2021; Received in final form - - 2021; Accepted - - 2021;
Available online - - 2021

Abstract

Monitoring river water level is of great importance to understand hydrological and hydraulic processes and evaluate flood and landslide risk. This paper proposes a method for estimating river water levels under bridges using multi-temporal high-resolution synthetic aperture radar (SAR) intensity images. Due to the side-looking characteristics of SAR data acquisitions, bridges crossing over rivers usually exhibit multiple bounce echoes in SAR images caused by the multipath scattering. The range difference of the multiple returns is proportional to the clearance between the water surface and the bridge. In this study, the water level oscillation of Yangtze River under Badong Yangzte River Bridge (China) was calculated by estimating the range pixel distances of the multiple bounces in ALOS-2 PALSAR-2 images using cross correlation algorithm. Besides, a linear correlation between the range pixel distance of the multiple bounces and in situ water level measurements was found, with a coefficient of determination equal to 0.9985. This relationship allowed estimating the river water level in each SAR acquisition, with an average error equal to -0.39 m and root mean square error of 0.51 m, and the elevation of the bridge, with an error of about 0.5 m, which is smaller than the theoretical uncertainty of the method (1.24 m). The obtained results show the efficiency of the method in estimating river water levels.

Keywords: river water level; high-resolution SAR image; multiple bounces; bridge; Yangzte River, China

1. Introduction

Monitoring river water level is of great importance because it can help to evaluate and assess flood and landslide risk and to observe and investigate the effects of global warming (Biondi et al., 2019). For these reasons, in the Yangtze River Basin of China, some institutions, such as Changjiang Maritime Safety Administration, Changjiang Waterway Bureau, and the China Three Gorges Corporation, have installed in situ gauges to monitor the water level of the river and the Three Gorges Reservoir several times per day.

Remote sensing has been widely used for monitoring the hydrometric level in previous studies. Altimetry remote sensing data from ENVISAT and ERS-2, Jason-1, ICESat, and GLAS were used to monitor the lake water level in Kivu (Africa), on the Tibetan Plateau, and in several Chinese large lakes (Omar et al., 2010; Zhang et al., 2011; Wang et al., 2013), and to estimate global mean sea level (Beckley et al., 2010). Synthetic aperture radar (SAR) images acquired by ENVISAT and Sentinel-1 missions were also used in estimating the water level. ENVISAT ASAR intensity images were combined with a digital elevation model (DEM) and hydraulic coherence concepts to estimate the Alzette River (Luxembourg) water level (Hostache et al., 2009). Sentinel-1 interferometry data were

*Corresponding author: Tel.: +39-049-827-9121; fax: +39-049-827-9134;
Email addresses: chenxue@cugb.edu.cn (Xue Chen), zhengyz@cugb.edu.cn (Yueze Zheng), pengjunhuan@163.com (Junhuan Peng), mario.floris@unipd.it (Mario Floris)

https://dx.doi.org/10.1016/j.jasr.xxxx.xx.xxx
0273-1177/

used in monitoring water level changes in Lake Kournas and Lake Agia (island of Crete, Greece) by detecting phase variations (Stavroulaki et al., 2017).

Several bridge detection and bridge parameters estimation methods based on SAR data have been developed. Soergel et al. (2008) observed that a bridge over water produces three parallel bright stripes in high resolution airborne interferometric SAR data due to multiple bounce effects. Cusson et al. (2012) showed the three returns of the Lions Gate Bridge (Canada) in RADARSAT-2 data acquired in Spotlight mode (1.6 m horizontal resolution). Zhang et al. (2015) analyzed the mechanism of multipath scattering of several structures, such as bridges, buildings, and oil tanks, in high-resolution TerraSAR-X images, and explored the potential to extract their geometry. Liu et al. (2016) proposed a method to estimate Golden Gate bridge (California, USA) parameters (e.g., height, width, thickness, and span) and the height of the bridge tower using high-resolution full polarimetric AIRSAR data.

During the past two decades, data collected by SAR sensors and processed through multi-temporal interferometric SAR techniques have become one of the most powerful tools for monitoring the land surface deformation, e.g., landslides. Monitoring river water levels using SAR images can help to synchronously investigate the relationship between water levels and instability of slopes or dams, especially in the Three Gorges area (Liao et al., 2012).

Previous studies on monitoring hydrometric levels using SAR images have been mainly focused on mapping the changes of lake surfaces. The multiple bounce scattering phenomenon of bridges in SAR images was explained more than 10 years ago (Soergel et al., 2008), and the theory of multiple bounce scattering has been used for describing the geometry of SAR acquisitions or detecting structures in the following years. Low attention has been paid to the river water level monitoring using bridge in SAR images. The water level oscillation can cause changes in the pixel locations of multiple bounces in SAR images. The developing coregistration methods of the SAR images can achieve a sub-pixel accuracy of offset, which facilitates the measurement of the changes of the pixel locations. Biondi et al. (2019) made the first attempt to use SAR images to estimate the hydrometric level. They proposed to use a sub-pixel offset tracking technique to estimate the hydrometric levels and applied this technique in the Po and Tiber rivers (Italy) using COSMO-SkyMed data, where the multiple bounces can hardly be distinguished.

This paper proposes a method for estimating the river water level using the backscattering of bridges in multi-temporal high-resolution SAR images. The method was tested in monitoring river levels under the Badong Yangzte River Bridge. To this end, L-band PALSAR-2 images acquired by the ALOS-2 mission and in situ water level measurements of the Three Gorges Reservoir, located nearby the bridge, were used. An equation, correlating the range pixel distances between multiple bounces produced the bridge in the SAR images and water levels, was derived. After calculating the range pixel distances using the cross correlation algorithm adopted in the SAR images coregistration, the water level oscillation was estimated. Furthermore, a linear regression of the pixel distances vs. the in situ water levels was performed, and the coefficients of the equation were obtained. By using the proposed equation, the river water level can be estimated from each SAR acquisition by calculating the range pixel distances of multiple bounces using cross correlation algorithm.

2. Methodology

In this section, the geometric models and mathematical expressions to measure the river water level using SAR images, are described. If the orientation of a bridge is not perpendicular to the orbit of the satellite, in high-resolution SAR images three bright parallel stripes are present, which represent: the direct backscatter from the bridge, the double bounce reflection between the bridge and water or vice versa, and the triple bounce reflection between the water, the lower part of the bridge, and the water again (Fig. 1). This phenomenon is due to the relative positions of the bridge, the satellite, and the water level, the reflection and refraction of the microwave, and the geometry of the SAR acquisition. The pixel distance between the direct and the other two reflections depends on the clearance between the bridge and the water surface.

The range pixel distance between the first (direct reflection) and second stripes (double bounce) in a bridge SAR image is influenced by the width of the structure, while the range pixel distance between the first and third stripes (triple bounce) is influenced by its thickness (see Fig. 1). For simplifying the algorithm, the width and thickness of the bridge were not taken into account in this study, but they should be considered in the case of wide, thick, and structurally complex bridges.

In a single look complex (SLC) SAR image, the range distance between the first and the third stripes (P1 - P3 in Fig. 1), equals to $N_{triple}R_{spacing}$, where N_{triple} is the number of pixels between the stripes in the range direction, and $R_{spacing}$ is the range pixel spacing. The location of a target in a SAR image is determined by the signal transmission distance between the radar antenna and the target. In this study, the range distance between the first and the third stripes is due to the difference in the signal transmission distances of the direct reflection and the triple bounces, which is $XW + WB = XW + WB' = BB' \cos\theta_{inc}$, where BB' is twice the difference between the bridge elevation (H_{bridge}) and water surface elevation (H_{water}), and θ_{inc} is the incident angle of the SAR sensor. Therefore, the relationship between the H_{water} and N_{triple} can be approximately expressed as follows:

$$N_{triple}R_{spacing} = 2(H_{bridge} - H_{water})\cos\theta_{inc} \quad (1)$$

N_{triple} can be calculated from the SAR image using cross correlation algorithm to obtain a sub-pixel offset. $R_{spacing}$ and θ_{inc} are usually provided in the SAR parameter file.

From equation (1), the river level H_{water} can be expressed as follows:

$$H_{water} = -\frac{R_{spacing}}{2\cos\theta_{inc}}N_{triple} + H_{bridge} \quad (2)$$

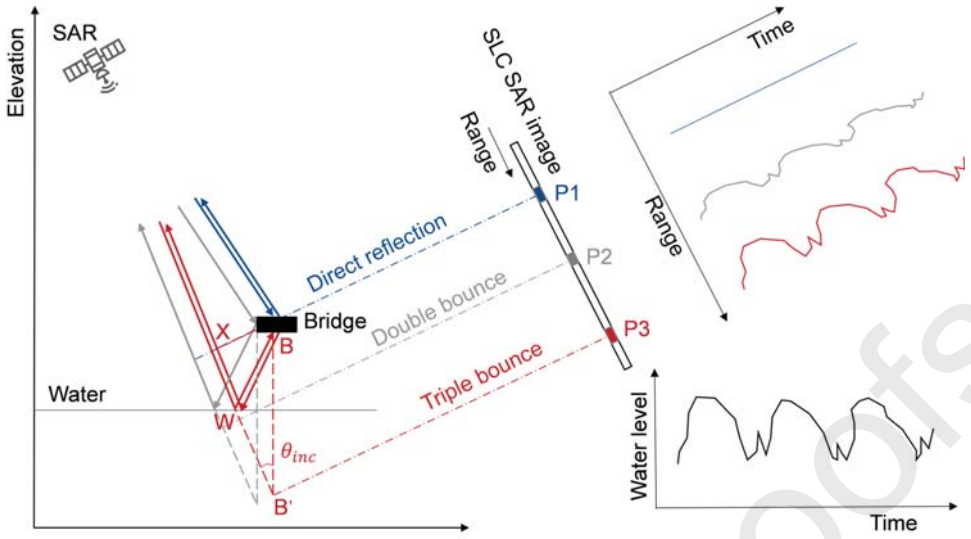

Fig. 1. Scheme of the multiple bounces produced by a bridge over the water.

To obtain the water level, three cases can occur, depending on the availability of information:

a. if H_{bridge} and in situ water level measurements are unknown, the river water oscillation can be calculated from all the available SAR images using equation (2);

b. if H_{bridge} is unknown, but in situ water level measurements are available, H_{bridge} can be estimated from equation (2). Alternatively, H_{bridge} and the coefficient $-R_{spacing}/(2\cos\theta_{inc})$ can be estimated through two or more in situ water level measurements using linear regression;

c. if H_{bridge} is known, H_{water} can be easily calculated from each SAR image.

In all the above-listed cases, multi-temporal high-resolution SAR images can allow monitoring the oscillation of water level. If two or more in situ water level measurements are available, bridge elevation can be estimated, and then the water level elevation can be calculated through SAR images.

The range pixel distance between the direct reflection and the triple bounce can be calculated based on the cross correlation function of the image intensity (Li & Goldstein, 1990). This function is used in the SAR image coregistration step in GAMMA (Wegmüller & Werner, 1997) software and it allows obtaining the sub-pixel offset.

In this study, we have considered the situations a and b, where both the bridge elevation and the in situ water levels are unknown (case a) and the bridge elevation is unknown but in situ water levels at the time of SAR acquisitions are available (case b). In case a, the relative position of the water level is calculated from the SAR images. In case b, the linear correlation function between range pixel distances and in situ water levels was calculated. Then, the parameters of the function were used to solve equation (2), being the slope of the linear fit equal to $-R_{spacing}/(2\cos\theta_{inc})$ and the intercept equal to H_{bridge}. By this method, the river water level can be estimated from any SAR image where the multiple bounces are distinguishable.

3. Study Area and Data Sources

The study area is located at the Three Gorges in the middle of the Yangtze River in Badong county, Hubei Province, China (Fig. 2). The Three Gorges were formed by the deep incision of Paleozoic and Mesozoic limestones. The highest elevations are 1000 - 2000 m and the river is at 100 - 300 m, the slope gradient range from 30° to 50°. The climate is subtropical monsoon with plentiful rainfall and high mean air temperature and humidity. The mean annual air temperature is 17.4°C and the mean annual rainfall is 1130 mm. The wet season, with about 70% of the annual precipitation, is in spring - summer (May - September). The Yangtze is the longest river in China (6300 km), the mean annual runoff is 450.5×10^9 m^3 and the mean annual discharge is 14300 m^3/s. The highest rates of level rise and level fall, recorded by the Yunyang station, are 6.73 m/day and 3.4 m/day, respectively. The oscillation of the river level induces a serious impact on the stability of bank slopes (Highland, 2008). Badong Yangtze River Bridge is the closest upstream bridge to the Three Gorges Reservoir with a distance of about 70 km (Fig. 2a). It consists of two planes of cables connected to a concrete A-frame tower with a total length of 908 m and a main span of 388 m (Fig. 2d). The bridge was constructed 147 m above the original river before the creation of the Three Gorges reservoir.

SAR images of the bridge acquired from COSMO-SkyMed, Sentinel-1A, and PALSAR-2 satellites are shown in Fig. 3. COSMO-SkyMed operates at X-band (wavelength ≈ 3.13 cm) and thus the image exhibits a quite high speckle noise. Even though the image has a high resolution with a range pixel spacing of about 0.95 m, the multiple bounce scattering of the bridge cannot be clearly identified. The bridge can be detected in the Sentinel-1A image (C-band, wavelength ≈ 5.55 cm), but the multiple bounces are not evident due to the noise, the range pixel spacing (2.32 m), and the rather large azimuth pixel spacing (13.98 m). In the case of PALSAR-2, thanks to the operating L-band (wavelength ≈ 23.86 cm) and the high reso-

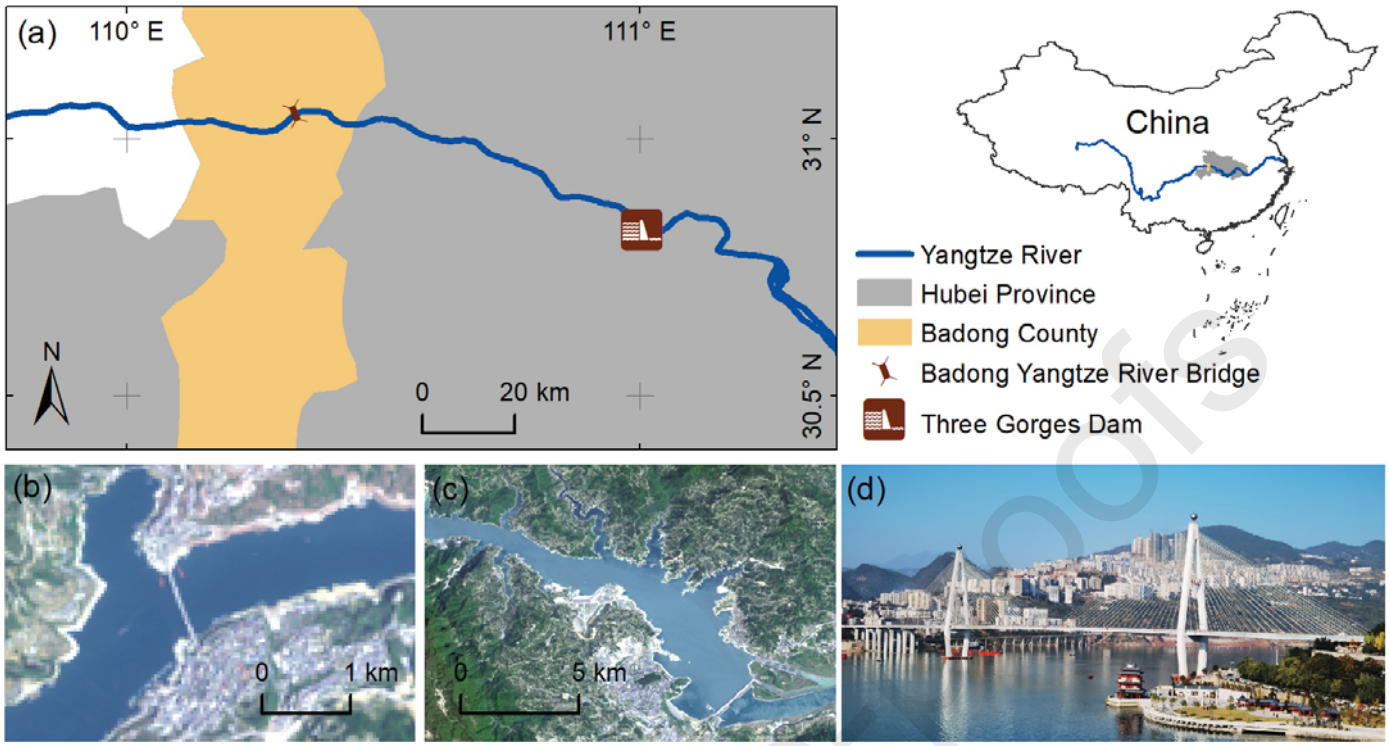

Fig. 2. Location of the study area (a) and satellite imagery of the Badong Yangtze River Bridge (b) and the Three Gorges Reservoir (c). (d) Photo of the Badong Yangtze River Bridge. Basemap credit: Landsat 8 OLI/TIRS images from U.S. Geological Survey dated April 27, 2020.

lution of the image (range pixel spacing ≈ 1.43 m), the bridge and the multiple bounces can be detected and analyzed.

Twenty-two PALSAR-2 ascending images spanning from August 15, 2016 to October 9, 2017, were considered in this study. The three parallel bright stripes in Fig. 3c represent the multiple bounce reflections caused by the bridge over the water. The changes in the clearance between the bridge and the water surface cause the variation of pixel location of the second and third stripes (from left to right, in right looking SAR images) and, consequently, the variation in the range pixel distance between the stripes. Taking into account the data acquisition geometry (incident angle = 32.4°) and the range and azimuth pixel spacings (1.43 m and 1.82 m), the ratio of the ground range and azimuth pixel spacing is $1.43/\sin(32.4°)/1.82 = 1.466$. This ratio means that the images have an approximate square pixel spacing and the bridge can be clearly identified without multi-looking processing.

Regarding the river water level, the in situ measurements of the Three Gorges Reservoir hydrometric level in Wusong elevation datum, collected by the China Three Gorges Corporation (https://www.ctg.com.cn), were used. The first water impoundment of the artificial reservoir was on June 1, 2003, then the water level reached an elevation of 135 m (June 15, 2003), 156 m (October 27, 2006), and 172.8 m (November 10, 2008). The current mean elevation is 160 m above sea level (a.s.l.) with an oscillation of about 10 m and it is measured four times per day, every six hours starting from 2 a.m.

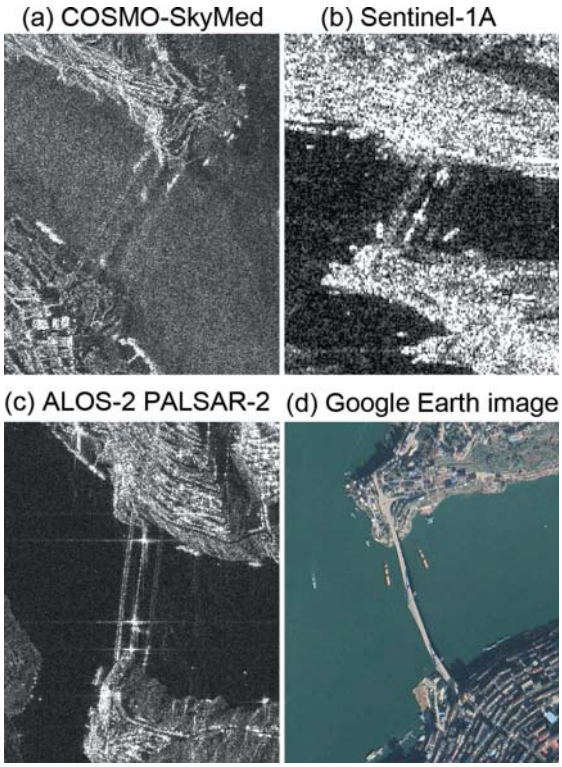

Fig. 3. SAR images of the Badong Yangtze River Bridge, acquired in right-looking mode by COSMO-SkyMed (a), Sentinel-1A (b), and ALOS-2 (c) satellites. (d) Google Earth image of the bridge.

Table 1. Comparison between estimated and measured river water level oscillation.

Date	N_{triple}	$H_{water}^{estimated}$ - H_{bridge} (m)	Estimated oscillation (m)	$H_{water}^{measured}$ (m)	Measured oscillation (m)	Difference between estimated and measured oscillation (m)
Aug 15, 2016	78.81	-66.74	-	145.63	-	-
Aug 29, 2016	77.27	-65.44	1.30	146.94	1.31	-0.01
Sep 12, 2016	74.35	-62.97	3.78	148.91	3.28	0.50
Sep 26, 2016	62.18	-52.66	14.09	159.45	13.82	0.27
Oct 10, 2016	55.93	-47.37	19.38	166.09	20.46	-1.08
Oct 24, 2016	48.56	-41.13	25.62	171.95	26.32	-0.70
Dec 19, 2016	46.89	-39.71	27.03	172.95	27.32	-0.29
Jan 30, 2017	50.23	-42.54	24.20	169.75	24.12	0.08
Feb 13, 2017	52.91	-44.81	21.94	168.12	22.49	-0.55
Feb 27, 2017	53.23	-45.08	21.67	167.25	21.62	0.05
Mar 13, 2017	55.21	-46.76	19.98	165.97	20.34	-0.36
Mar 27, 2017	56.58	-47.92	18.83	164.88	19.25	-0.42
Apr 10, 2017	59.11	-50.06	16.68	162.36	16.73	-0.05
Apr 24, 2017	61.90	-52.42	14.32	161.00	15.37	-1.05
May 8, 2017	62.64	-53.05	13.70	159.42	13.79	-0.09
May 22, 2017	70.60	-59.79	6.95	152.84	7.21	-0.26
Jun 5, 2017	76.88	-65.11	1.63	147.56	1.93	-0.30
Aug 14, 2017	77.19	-65.37	1.37	147.25	1.62	-0.25
Aug 28, 2017	73.86	-62.56	4.19	150.38	4.75	-0.56
Sep 11, 2017	64.20	-54.37	12.37	158.31	12.68	-0.31
Sep 25, 2017	57.05	-48.32	18.42	165.08	19.45	-1.03
Oct 9, 2017	48.90	-41.41	25.33	172.05	26.42	-1.09

N_{triple} is the range pixel distance between the direct reflection and the triple bounce. $H_{water}^{estimated}$ is the estimated water level. H_{bridge} is the elevation of the bridge. $H_{water}^{measured}$ is the in situ water level measurement.

4. Results

In each PALSAR-2 image, the first stripe on the left is the direct reflection of the bridge, whose position is fixed in the entire SAR dataset. The position of the second and third stripes changes over time due to the variation of the river water level. The range pixel distances between the direct reflection and the triple bounces (N_{triple}) estimated by cross correlation algorithm are listed in Table 1.

In the case the elevation of the bridge (H_{bridge}) and in situ water level measurements are unknown (case a), the relative position of the water level from the bridge was estimated by the range pixel distance in each SAR image, using equation (2), with $R_{spacing}$ equals to 1.43 and θ_{inc} equals to 32.4. In this case, only the water level oscillation can be obtained (Table 1). To evaluate the accuracy of the estimated oscillations, the in situ measurements of the Three Gorges Reservoir, collected at the closest time of the SAR acquisitions, were considered. Because the PALSAR-2 acquisition time is around 4:34 p.m. in coordinated universal time, which is 8 hours behind Beijing time, the first measurements (2:00 a.m.) of the day after the acquisition were used. The root mean square error (RMSE) value between the estimated and in situ measurements was calculated as follows:

$$RMSE = \sqrt{\frac{1}{N}\sum_{i=1}^{N}\left(X_i^{estimated} - X_i^{measured}\right)^2} \quad (3)$$

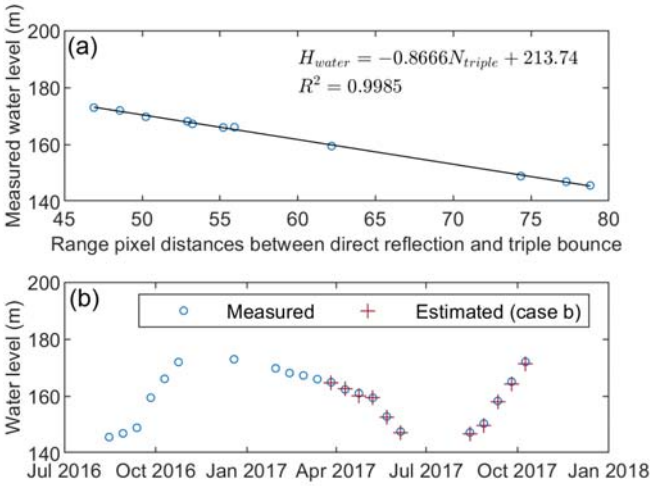

Fig. 4. Estimated river water level. (a) Relationship between range pixel distances and in situ water level measurements of the first 11 SAR acquisitions. (b) Estimated water level from the last 11 SAR acquisitions.

where the $X_i^{estimated}$ is the estimated water level oscillation at the ith SAR acquisition, $X_i^{measured}$ is the oscillation calculated by the in situ measurements, and N is the number of observations. The maximum, mean, and minimum differences between estimated and measured oscillations are -1.09, -0.36, and -0.01 m, and the RMSE is 0.55 m.

In the case H_{bridge} is unknown, but in situ water level mea-

Table 2. Comparison between estimated and measured river water levels.

Date	N_{triple}	$H_{water}^{measured}$ (m)	$H_{water}^{estimated}$ (m)	$H_{water}^{estimated} - H_{water}^{measured}$ (m)
Mar 27, 2017	56.58	164.88	164.71	-0.17
Apr 10, 2017	59.11	162.36	162.51	0.15
Apr 24, 2017	61.90	161.00	160.10	-0.90
May 8, 2017	62.64	159.42	159.46	0.04
May 22, 2017	70.60	152.84	152.56	-0.28
Jun 5, 2017	76.88	147.56	147.11	-0.45
Aug 14, 2017	77.19	147.25	146.85	-0.40
Aug 28, 2017	73.86	150.38	149.73	-0.65
Sep 11, 2017	64.20	158.31	158.11	-0.20
Sep 25, 2017	57.05	165.08	164.30	-0.78
Oct 9, 2017	48.90	172.05	171.36	-0.69

N_{triple} is the range pixel distance between the direct reflection and the triple bounce. $H_{water}^{estimated}$ is the estimated water level. $H_{water}^{measured}$ is the in situ water level measurement.

surements are available (case b), the H_{water} can be estimated from SAR images. To this end, the first 11 SAR acquisitions were considered. The relationship between the range pixel distance of multiple bounces of the acquisitions (N_{triple}) and in situ river water level (H_{water}) is shown in Fig. 4a. A linear correlation was found with the coefficient of determination 0.9985, which can be expressed as follows:

$$H_{water} = -0.8666 N_{triple} + 213.74 \quad (4)$$

Comparing equations (4) and (2), H_{water} is proportional to N_{triple}. The slope (-0.8666) is $-R_{spacing}/2\cos\theta_{inc}$ and the intercept (213.74) is H_{bridge}. Based on this linear correlation, the water level at each SAR acquisition can be estimated from the range pixel distance using equation (4).

The last 11 SAR acquisitions were used for cross-validation of the method. The comparison between estimated and measured water levels is shown in Table 2 and Fig. 4b. The maximum, mean, and minimum differences are -0.90 m, -0.39 m, 0.04 m, and the RMSE is 0.51 m.

5. Discussion

The accuracy of the results can be affected by some uncertainty deriving from the pixel spacing. Especially when the structure of the bridge is complex or the wavelength/resolution is not good enough, the sub-pixel distance can hardly be estimated through the cross correlation function. But the range pixel distance can be obtained by counting the visible stripes with pixel scale. In the case of the estimation of bridge elevation, according to the error propagation law, the uncertainty is:

$$\delta H_{bridge} = \left| \left(\frac{R_{spacing}}{2\cos\theta_{inc}} N_{st} + H_{water} \right)' \right| \delta N_{triple} \quad (5)$$

In our case study, δN_{triple} = 1.43 m, which equals to the range spacing, and thus δH_{bridge} = 1.24 m, indicating that the measurement uncertainty of bridge elevation is 1.24 m, without considering the bridge structure.

The estimated bridge elevation has been calculated referring to the China 1985 national height datum and it is 213.74 m. According to our measurement, the bridge elevation in the world geodetic system 1984 (WGS84) system is 186.44 m. The Geoid height is about -24.75 m in the earth gravitational model 2008 (EGM2008). Considering that the China 1985 national height datum is 21.0 cm higher than the global height datum (Li et al., 2017), and the Wusong elevation datum is 1.84 m higher than the China 1985 national height datum (Yan et al., 2008), the bridge elevation in Wusong elevation datum is 186.44+24.75+0.21+1.84 = 213.24 m. Then, the error of the measured elevation is 0.5 m, within the measurement uncertainty.

The error in the estimation of the bridge elevation was possibly due to the main assumptions of the proposed method. First, the dimensions of the bridge (width and thickness) were not taken into account to simplify the geometry modeling. Second, the water level measurements are not accurate because they were collected at the Three Gorges Reservoir, 70 km far from the bridge, and 1 hour and 26 minutes after the SAR image acquisitions.

The water level oscillation and the range spacing (usually a little smaller than the resolution), are two key factors in the proposed method. Based on equation (2), image spacing can be expressed as follows:

$$R_{spacing} = -\frac{2\cos\theta_{inc}}{N_{triple}} H_{water} + \frac{2\cos\theta_{inc} H_{bridge}}{N_{triple}} \quad (6)$$

Considering equation (2), when the image spacing is equal to 1 m, water level oscillation higher than $1/(2\cos\theta_{inc})$ can be estimated from SAR images, i.e., if θ_{inc} is equal to 30°, the water level oscillation has to be higher than 0.5774 m. Similarly, considering the equation (6), when the oscillation is equal to 1 m, the range spacing has to be smaller than $2\cos\theta_{inc}$, i.e., if θ_{inc} is equal to 30°C, the range spacing has to be smaller than 1.732 m.

To show the influence of water level oscillation and pixel spacing in the application of the proposed method, two examples are reported (Fig. 5): the first regards the Deh Cho Bridge, located in Canada; the second the Carquinez Bridge, located in the United States. Figs. 5b and 5d show the uninhabited aerial vehicle synthetic aperture radar (UAVSAR) images of the two bridges. The slant range spacing is 1.666 m in single look format and 4.997 m in multilook format, and the incident angle varies from 20° to 60°. According to equation (2), water level oscillation higher than 0.886 - 1.666 m (single look) or 2.65 - 4.997 m (multilook),depending on the incidence angle, can be detected because they produce one pixel shift in the SAR image.

In the Deh Cho Bridge UAVSAR image (Fig. 5b), three bright stripes are visible, but they are not parallel: the range distance is maximum in the middle part of the bridge, where the elevation of the structure is higher. In this case, the relative elevation of the different sections of the bridge can be measured by geometric calculation. The position of the stripes does not change in the 4 UAVSAR images acquired from June

Fig. 5. Google map image and UAVSAR amplitude image of the Deh Cho Bridge, Canada (a, b) and the Carquinez Bridge, USA (c, d). (e) Location of the two bridges. UAVSAR images were extracted from the database available at https://uavsar.jpl.nasa.gov/.

2017 to September 2019 because the river water level oscillation was too small. The minimum, mean, and maximum water level observed at the MACKENZIE RIVER NEAR FORT PROVIDENCE hydrometric station (https://wateroffice.ec.gc.ca/) in the period 1983 - 2017 are 148.995 m, 151.045 m and 153.532 m, respectively.

The Carquinez Bridge consists of two bridges, and the western one produces three parallel stripes in the UAVSAR image (Fig. 5d). In the 32 available UAVSAR images acquired from March 2010 to February 2020, the changes in the positions of the stripes are less than one pixel in range direction, because also in this case the oscillation of the water level was too small. In this area, the water level is influenced by the tides, which are collected at the CROCKETT, CARQUINEZ STRAIT station (https://tidesandcurrents.noaa.gov/). During the acquisition period of the UAVSAR images, the maximum oscillation of the tide was 1.8 m, which is hard to cause the variation of stripes range distance in bridge SAR images.

The method proposed in this study allows monitoring the river water level using bridges in SAR images. It can be very useful in areas without water level monitoring stations and characterized by high hydrometric oscillations. Monitoring river oscillation is crucial for analyzing instability phenomena affecting the slopes due to variations in the seepage. The analysis of the uncertainty of the proposed method caused by the pixel spacing and water level changes is useful for the design of a new UAVSAR system.

6. Conclusions

In this study, we provide a method to measure the river water level based on the range pixel distance of multiple bounces produced by bridges in multi-temporal high-resolution SAR images. Using 22 ALOS-2 PALSAR-2 images, the relative water level changes of Yangtze River under Badong Yangzte River Bridge were calculated by estimating the range pixel distance (in sub-pixel scale) of the multiple bounces in the images through cross correlation algorithm. Using in situ water level measurements, a linear correlation between the range pixel distance of multiple bounces and the river water level was found. Based on this correlation, the river water level was estimated with a RMSE of 0.51 m, and the elevation of the bridge was obtained with an error about 0.5 m, within the theoretical uncertainty of the method. The range pixel spacing of SAR images is the main factor conditioning the reliability of the method because it limits the minimum variation of the water level that can be estimated. The proposed method is easy to use and and shows high efficiency, and it can be applied to different types of SAR data where the multiple bounces are visible. In the next future, we can expect the construction of more and more bridges which will allow analyzing different case studies to evaluate the performance of the method. Besides, thanks to the growing availability of high-resolution SAR data with a short revisit time and the development of target recognition algorithms, the method would be improved to measure small oscillation of water level.

References

Beckley, B., Zelensky, N., Holmes, S., Lemoine, F., Ray, R., Mitchum, G., Desai, S., & Brown, S. (2010). Assessment of the Jason-2 extension to the TOPEX/Poseidon, Jason-1 sea-surface height time series for global mean sea level monitoring. *Marine Geodesy*, *33*(S1), 447–471. doi:10.1080/01490419.2010.491029.

Biondi, F., Tarpanelli, A., Addabbo, P., Clemente, C., & Orlando, D. (2019). Pixel tracking to estimate rivers water flow elevation using Cosmo-SkyMed synthetic aperture radar data. *Remote Sensing*, *11*(21), 2574. doi:10.3390/rs11212574.

Cusson, D., Ghuman, P., Gara, M., & McCardle, A. (2012). Remote monitoring of bridges from space. *Anais do*, *54*, 1–25.

Highland, L. M. (2008). Geographical overview of the Three Gorges Dam and Reservoir, China - Geologic hazards and environmental impacts. *U. S. Geological Survey*, (p. 46). doi:10.3133/ofr20081241.

Hostache, R., Matgen, P., Schumann, G., Puech, C., Hoffmann, L., & Pfister, L. (2009). Water level estimation and reduction of hydraulic model calibration uncertainties using satellite SAR images of floods. *IEEE Transactions on Geoscience and Remote Sensing*, *47*(2), 431–441. doi:10.1109/tgrs.2008.2008718.

Li, F. K., & Goldstein, R. M. (1990). Studies of multibaseline spaceborne interferometric synthetic aperture radars. *IEEE Transactions on Geoscience and Remote Sensing*, *28*(1), 88–97. doi:10.1109/36.45749.

Li, J., Chu, Y., & Xu, X. (2017). Determination of Vertical Datum Offset between the Regional and the Global Height Datum. *Acta Geodaetica et Cartographica Sinica*, *46*(10), 1262. doi:10.11947/j.AGCS.2017.20170538.

Liao, M., Tang, J., Wang, T., Balz, T., & Zhang, L. (2012). Landslide monitoring with high-resolution SAR data in the Three Gorges region. *Science China Earth Sciences*, *55*(4), 590–601. doi:10.1007/s11430-011-4259-1.

Liu, G., Zhang, J., Zhang, X., Meng, J., & Wang, G. (2016). A parameter inversion for sea bridge based on high-resolution polarimetric synthetic aperture radar. *Acta Oceanologica Sinica*, *35*(7), 68–75. doi:10.1007/s13131-016-0912-z.

Omar, M., Umaru, G., McArd, J., Florent, L. et al. (2010). Water level monitoring using radar remote sensing data application on Lake Kivu. *African Journal of Science and Technology*, *11*(1), 17–30. doi:10.1016/j.pce.2009.06.008.

Soergel, U., Cadario, E., Thiele, A., & Thoennessen, U. (2008). Feature extraction and visualization of bridges over water from high-resolution InSAR data and one orthophoto. *IEEE Journal of Selected Topics in Applied Earth Observations and Remote Sensing*, *1*(2), 147–153. doi:10.1109/jstars.2008.2001156.

Stavroulaki, E., Alexakis, D. D., & Tsanis, I. K. (2017). Monitoring water level using Sentinel-1 interferometric synthetic aperture radar (InSAR) images. In *EGU General Assembly Conference Abstracts* (p. 17521).

Wang, X., Gong, P., Zhao, Y., Xu, Y., Cheng, X., Niu, Z., Luo, Z., Huang, H., Sun, F., & Li, X. (2013). Water-level changes in China's large lakes determined from ICESat/GLAS data. *Remote Sensing of Environment*, *132*, 131–144. doi:10.1016/j.rse.2013.01.005.

Wegmüller, U., & Werner, C. (1997). Gamma SAR processor and interferometry software. *ESA SP (Print)*, (pp. 1687–1692).

Yan, G., Lin, W., Zhou, F., & Zeng, N. (2008). Monitoring dynamics of grassland vegetation in Poyang Lake national nature reserve, using MODIS imagery. In *The International Archives of the Photogrammetry, Remote Sensing and Spatial Information Sciences* (pp. 1337–1342).

Zhang, G., Xie, H., Kang, S., Yi, D., & Ackley, S. F. (2011). Monitoring lake level changes on the Tibetan Plateau using ICESat altimetry data (2003–2009). *Remote Sensing of Environment*, *115*(7), 1733–1742. doi:10.1016/j.rse.2011.03.005.

Zhang, Y., Ding, C., Qiu, X., & Li, F. (2015). The characteristics of the multipath scattering and the application for geometry extraction in high-resolution SAR images. *IEEE Transactions on Geoscience and Remote Sensing*, *53*(8), 4687–4699. doi:10.1109/tgrs.2015.2406793.